Structure-Based Drug Design

Application and Limitations of X-ray Crystallographic Data in Structure-Based Ligand and Drug Design

Andrew M. Davis, Simon J. Teague, and Gerard J. Kleywegt*

Keywords:
drug design · protein models · protein structures · X-ray crystallography

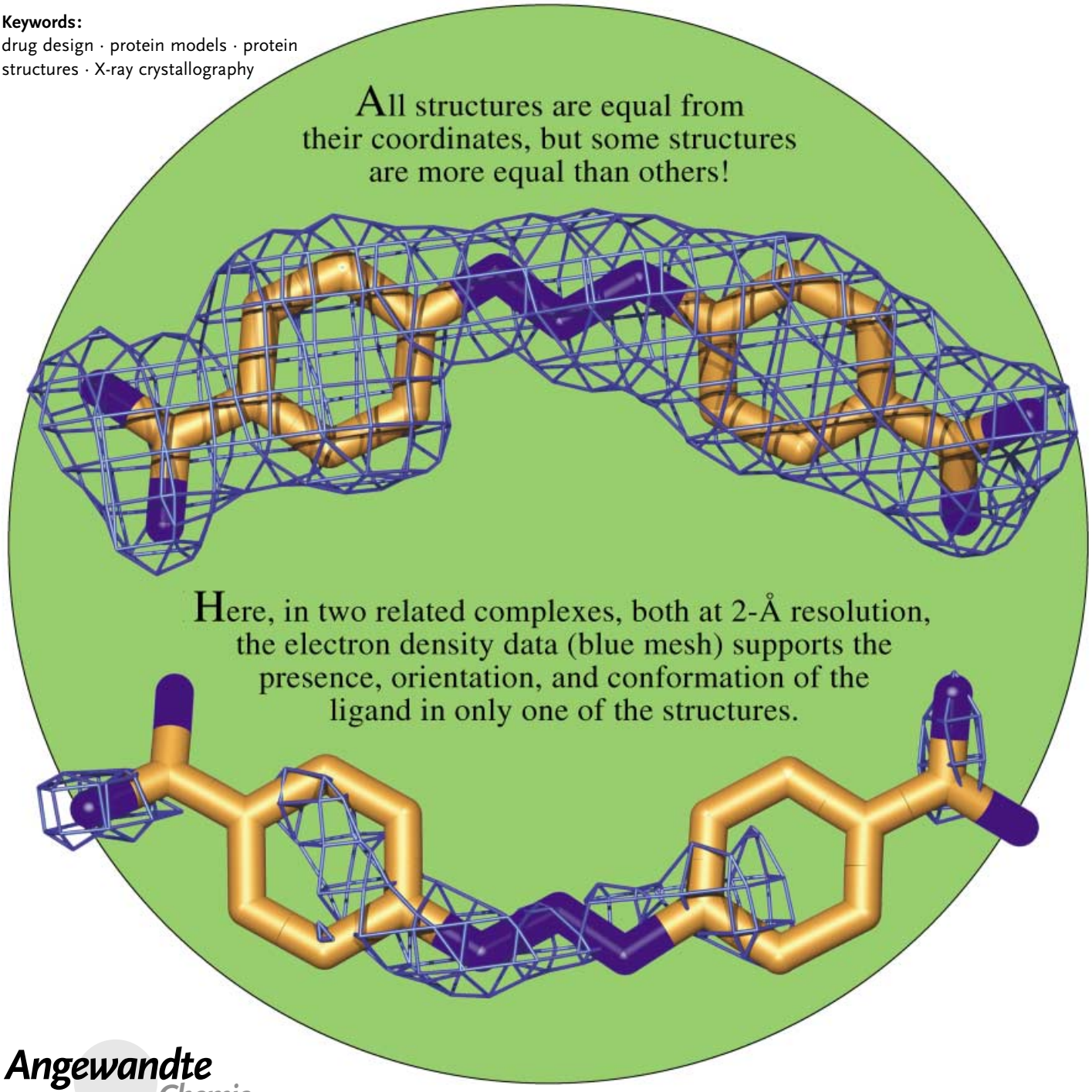

Angewandte Chemie

DOI: 10.1002/anie.200200539

Structure-based design usually focuses upon the optimization of ligand affinity. However, successful drug design also requires the optimization of many other properties. The primary source of structural information for protein–ligand complexes is X-ray crystallography. The uncertainties introduced during the derivation of an atomic model from the experimentally observed electron density data are not always appreciated. Uncertainties in the atomic model can have significant consequences when this model is subsequently used as the basis of manual design, docking, scoring, and virtual screening efforts. Docking and scoring algorithms are currently imperfect. A good correlation between observed and calculated binding affinities is usually only observed only when very large ranges of affinity are considered. Errors in the correlation often exceed the range of affinities commonly encountered during lead optimization. Some structure-based design approaches now involve screening libraries by using technologies based on NMR spectroscopy and X-ray crystallography to discover small polar templates, which are used for further optimization. Such compounds are defined as leadlike and are also sought by more traditional high-throughput screening technologies. Structure-based design and HTS technologies show important complementarity and a degree of convergence.

From the Contents

1. Introduction

The use of protein structure information in drug discovery is often termed structure-based design, and it encompasses a number of technologies (Table 1). Although many pharmaceutical companies invested heavily in structure-based design in the 1980s, by the 1990s it appeared passé, as the industry focused upon the new great hope for drug discovery—modern high-throughput screening (HTS) of compounds produced by combinatorial chemistry.

Presently, however, structure-based design is undergoing a renaissance. This renewed interest has a number of drivers. Advances in molecular biology have made possible the reliable production of homogeneous, natural or modified proteins suitable for rapid, iterative crystallographic and NMR studies of ligand–protein complexes. Mutagenesis of these cloned and expressed proteins allows direct probing of ligand–receptor interactions.[28] A better understanding of the energetics of ligand–receptor interactions has been derived from a combination of mutagenesis with classical physical-organic chemistry investigations,[29] X-ray crystallography,[13] and thermodynamic measurements.[30] The hardware and software available to computational chemists has improved dramatically and so has the quality and speed of ligand docking algorithms. This has taken the subjectivity out of the placement of virtual structures into a protein's active site. It has also opened up the possibility of using structural information in lead generation. Virtual screening of large collections of compounds, or even larger virtual libraries, can be undertaken almost routinely with tools like DOCK,[6] GOLD,[8] FLEX-X,[7] and SLIDE.[23] Likewise, the prediction of physical properties from structures has improved greatly. Currently much emphasis is being placed upon computationally filtering by physical properties to remove nondruglike compounds[31,32] in order to frontload HTS or to guide library design.

The revolution in computer technology is showing no signs of slowing down, with current Linux farms allowing many hundreds of parallel calculations to be made in acceptable timescales. By means of Seti technology[33] over PC networks, researchers at the University of Oxford are using 1.2 million household PCs to screen 3.2 billion virtual structures in 13 protein active sites in a search for novel anticancer agents.[34] Another important driver is the increasingly high cost and competitiveness of drug discovery and development. This requires the process to be not only faster, but also smarter.[35] Although HTS is useful in the hunt for novel leads, screening of small subsets chosen by virtual screening can be very useful when the structure of the protein is available. This is especially true when other factors preclude HTS of the entire company file. The possibilities for successful structure-based design have never been greater.

[*] Dr. A. M. Davis, Dr. S. J. Teague
AstraZeneca R&D Charnwood
Bakewell Road, Loughborough
Leicestershire LE11 5RH (United Kingdom)
Fax: (+44) 150-964-5576
E-mail: andy.davis@astrazeneca.com
Dr. G. J. Kleywegt
Department of Cell and Molecular Biology
Uppsala University, Biomedical Centre
Box 596, SE-75124 Uppsala (Sweden)

 DOI: 10.1002/anie.200200539

Table 1: A selection of current structure-based design technologies.

Technology	Objective	Programs/Tools
X-ray crystallography Protein NMR spectroscopy Homology modeling	Protein structure generation	O,[1] CNS,[2] X-PLOR,[3] CCP4, [4] MODELLER[5]
Ligand docking	Prediction of bound ligand conformation	Manuel docking, DOCK,[6] Flex-X[7] GOLD[8]
Receptor interaction mapping	Ligand optimization	GRID,[9] MCSS, [10] RELIBASE,[11] SUPERSTAR[12]
Scoring	Affinity prediction	GLIDE, GOLD, LUDI,[13] DOCKSCORE,[14] SmoG2001[15]
3D QSAR	Affinity prediction	CATALYST,[16] COMFA,[17] GOLPE[18]
De novo design	Automated ligand design	LEAPFROG,[19] LUDI CombiSMoG,[20] SPROUT[21]
Pharmacophore searching	Potential lead retrieval from real or virtual databases	CATALYST, UNITY[22]
Virtual screening	Lead selection from a virtual library guided by a docking into a protein structure	DOCK, Flex-X, GLIDE GOLD, SLIDE[23]
Structure-based screening	Lead selection guided by direct observation of the ligand–protein interaction	SAR-by-NMR,[24] SHAPES,[25] CRYSTALLEAD,[26] high-throughput crystallography[27]

Structure-based design and the technologies listed in Table 1 are an extremely active area of research and have been extensively and frequently reviewed.[36–40] However, these new technologies may not suffice, since their successful application still has some severe limitations. The aim of structure-based design is the optimization of ligand potency, which is usually measured in a simple in vitro competitive inhibition or binding assay. However, the aim of all pharmaceutical research projects is the discovery of a candidate drug. Here, we highlight the distinction between ligand design and drug design, and illustrate the difference with case histories from studies on HIV-protease, neuraminidase, carbonic anhydrase, and renin inhibitors. In most cases the protein structure used in the structure-based design process has been determined by X-ray crystallography rather than NMR spectroscopy. The latter technique is limited by constraints on the molecular size of the protein and the requirement for multiple isotopic labeling. Since all the technologies listed in Table 1 depend upon protein structural information, we highlight some of the pitfalls and limitations in protein structure determination by X-ray crystallographic methods that might otherwise mislead the unwary user. Addressing these ambiguities may lead to further opportunities, which we highlight in this review.

2. Structure-Based Design of Ligands and Drugs

Structure-based design is often loosely termed structure-based drug design or rational drug design. Usually the processes described could be termed more accurately structure-based ligand design, since the objective is to optimize the potency of a ligand in a simple in vitro assay. Drug design requires optimization of many other properties including dissolution, absorption, metabolic stability, plasma protein binding, distribution, elimination, toxicological profile, cost of synthesis, and pharmaceutical

Simon Teague, born in 1959 in Worcester (UK), gained his PhD at the University of Nottingham in the group of Professor G. Pattenden. He carried out postdoctoral work with Professor A. I. Meyers at Colorado State University (USA). He is now a Principle Scientist at AstraZeneca R&D Charnwood (UK). His research interests are lead generation methodologies and the study of drug–receptor interactions.

Andy Davis, born in 1961 in Wells, Somerset (UK), gained his BSc degree from Imperial College, London, and his PhD at the University of Huddersfield with Professor M. I. Page for studies on the kinetics and mechanism of rearrangements of penicillins. He is now Associate Director of Physical Chemistry at AstraZeneca R&D Charnwood. His interests are the energetics of ligand–receptor interactions, QSAR methods, and the cooperative application of physical-organic and computational chemistry to drug discovery.

properties. Structure-based design has already contributed to the discovery of a number of very important drugs such as the peptidomimetic HIV-protease inhibitors nelfinavir (**1**), saquinavir (**2**), ritonavir (**3**), indinavir (**4**), amprenavir (**5**), and lopinavir (**6**, Scheme 1).

Peptidomimetic HIV-protease inhibitors are already in clinical use. Although these drugs are successful commercially and clinically, they have distinct therapeutic limitations, and the search for more effective inhibitors continues. Poor bioavailability has been reported for saquinavir, and variable bioavailability for a number of members of this class of agents. They also suffer from moderate to high clearance, nonlinear phamacokinetics, and very significant interactions with other drugs. In addition they are substrates for p-glycoprotein efflux proteins. These effects are very significant clinically since the drugs may be excluded from certain organs, which provides the virus with a safe haven[41,42] from which it may reemerge. The market for HIV proteases may well accept improved inhibitors with more favorable absorption, distribution, metabolism, and elimination (ADME) properties. Agents with improved properties sometimes displace first generation drugs, as was the case for the antihypertensive calcium channel antagonist amlodipine, which largely replaced nifedipine.

The HIV-protease inhibitor DMP323 (**7,** IC_{50} = 0.031 nM) was discovered by structure-based design (Scheme 2) and progressed into clinical development. Its development illustrates a number of important and recurring themes[43,44] in the progress from a ligand to an effective drug. The clinical trials of **7** were terminated due to poor bioavailability caused by low solubility and metabolic instability associated with the benzyl alcohol groups. An excellent ligand proved to be a suboptimal drug. A second clinical candidate entered development, DMP450 (**8**), which displayed improved affinity along with better solubility and good bioavailability in humans. In phase II DMP450 was found to have only modest potency in patients. Dupont–Merck reentered the discovery phase of the project, again utilizing a structure-based approach, but this time including a potency assay in whole plasma. This aimed to address the deficiency of DMP450, which was perceived to be its high plasma protein binding. Plasma protein binding affects all drugs in vivo and largely depends upon lipophilicity and charge. It modulates the concentration of the drug in free plasma, which drives efficacy. Dupont–Merck's latest clinical candidates are DMP 850 (**9**) and DMP851 (**10,** Scheme 2), both of which have improved potency in whole blood , as well as increased solubility and bioavailability. The second and third phases of the program were focused upon incorporating druglike properties whilst maintaining ligand potency.

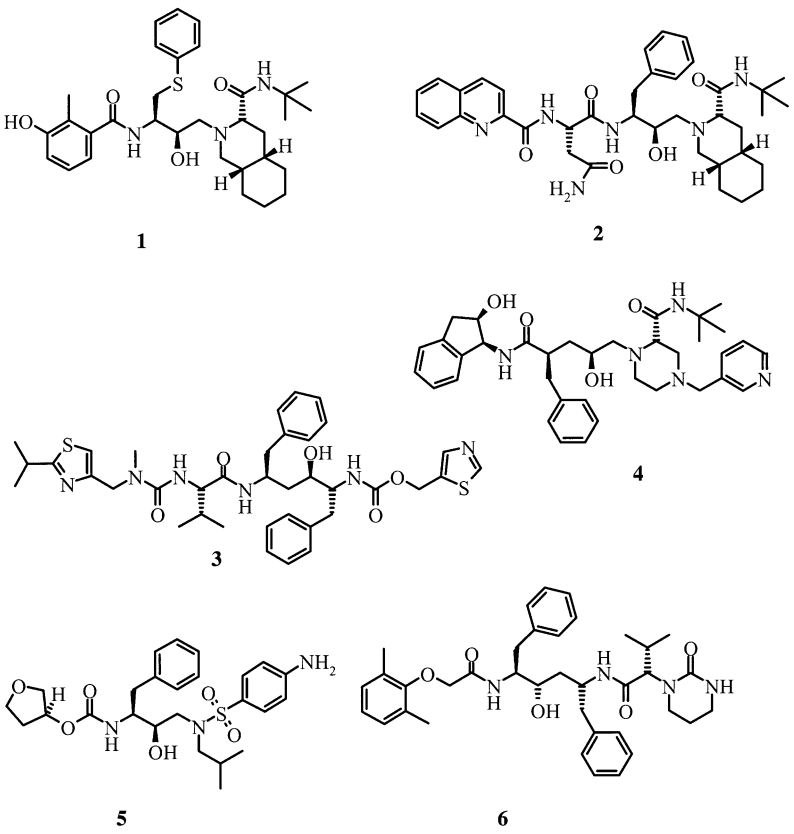

Scheme 1. The peptidomimetic HIV-protease inhibitors nelfinavir (**1**), saquinavir (**2**), ritonavir (**3**), indinavir (**4**), amprenavir (**5**), and lopinavir (**6**).

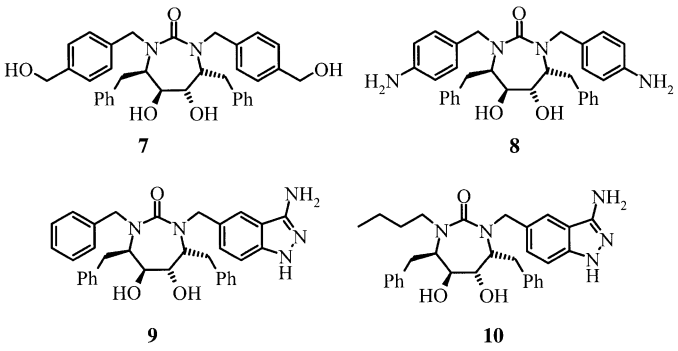

Scheme 2. The HIV-protease inhibitors DMP323 (**7**), DMP450 (**8**), DMP850 (**9**), and DMP851 (**10**).

Gerard J. Kleywegt obtained a degree in chemistry from the University of Leiden (The Netherlands) in 1986 and his doctorate from the University of Utrecht in 1991. After a short time with a commercial software company, he moved to Sweden to join Alwyn Jones's protein crystallography laboratory in Uppsala. He is currently working as an independent investigator at Uppsala University, and has been the coordinator of the Swedish Structural Biology Network (SBNet) since its inception in 1994. In 2001 he was awarded a research fellowship by the Royal Swedish Academy of Sciences.

Similar problems were also encountered with Pharmacia–Upjohn's pyrone sulfonamide inhibitors of HIV protease.[45] Broad screening of a "diverse" subset identified warfarin as an interesting but weak inhibitor. Similarity searching identified a related compound, phenprocoumon, as a potential

lead. The use of X-ray structural information led to PNU-103017 (**11**, Scheme 3), which although a potent HIV-protease inhibitor with excellent phamacokinetics, failed to demonstrate sufficient cellular activity due to its high plasma protein binding. Again, optimization aimed at reducing plasma protein binding and increasing potency resulted in an improved clinical candidate, tipranavir (**12**, Scheme 3).

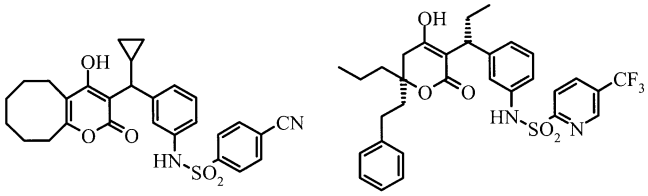

11 **12**

Scheme 3. The HIV-protease inhibitors PNU-103017 (**11**) and tipranavir (**12**).

A second case study is provided by the search for neuraminidase inhibitors. Neuraminidase has been an important target for antiinfluenza therapy for many years. Mark von Itzstein and his group at Monash University used the program GRID in an attempt to identify binding hotspots in the active site of neuraminidase to guide compound design.[46] GRID suggested replacement of the 4-hydroxy group in **13** by a basic moiety (Scheme 4). Replacement of the hydroxy by the basic guanidinyl group resulted in a 5000-fold increase in affinity. This compound, zanamivir (**14**), was subsequently developed by GlaxoSmithKline and marketed as the first neuraminidase-based antiinfluenza drug, Relenza.

Zanamivir is a very polar molecule and is dosed topically to the lung by means of dry-powder inhalation.[47] However, Gilead Pharmaceuticals were able to obtain sufficient potency without incorporation of either the strongly basic guanidine group or the polar glycerol side chain by replacement of the glycerol chain with a 1-ethylpropoxy group.[48] This group participates in favorable hydrophobic contacts and induces movements in protein side chains, which result in the formation of an additional salt bridge between Glu 276 and Arg 244. This design process resulted in oseltamivir carboxylate (**15**), a compound with more moderate polarity and charge. The zwitterionic parent is unsuitable as an oral drug, but the ethyl ester prodrug allows the compound to be absorbed orally. Oseltamivir is marketed by Hoffman–La Roche as Tamiflu. This was the first oral antiinfluenza drug, and in the first six weeks of sales in the USA Tamiflu took 40 % of the neuraminidase inhibitor market from Relenza.[49]

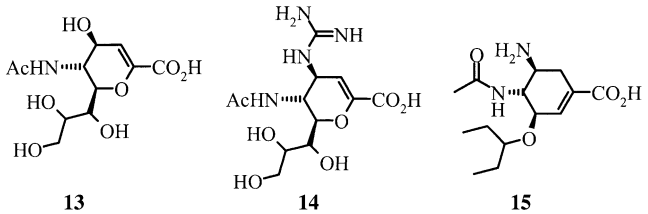

13 **14** **15**

Scheme 4. Neuraminidase inhibitors.

More balanced polarity, charge, and lipophilicity in Tamiflu resulted in a more acceptable physical property profile and considerable commercial success.

The search for renin inhibitors affords a third case study of the importance of considering ADME properties and the difference between ligands and drugs. Many of the world's pharmaceutical companies have attempted to discover renin inhibitors. The structure of murine renin became available in 1984[50] and that of the human renin in 1989.[51] Before 1989, structure-based design programs utilized homology models of renin based on the aspartyl peptidases endothiapepsin, penicillopepsin, and rhizopuspepsin. With the availability of high-resolution X-ray structures to guide compound design, it might have been expected that by now this target would have yielded a drug. But all these renin programs failed to discover low-molecular-weight agents. Potent ligands were developed but not drugs.[52] Further development of the compounds found was discontinued owing to variable bioavailability and/or excessive production costs. Availability of detailed structural information had not aided the rational design of potent inhibitors with an acceptable pharmacokinetic profile. However, the pharmaceutical industry has not given up on this target. Recently, researchers at Roche have described compound **16**,[53] a renin inhibitor in the nM-range, which was developed from the HTS hit **17** (26 μM, Scheme 5). With a molecular weight of 550 Da compound **16** is one of the smallest, most druglike ligands to have been discovered and is furthest from the peptidic ligands of the 1990s. Both the lead

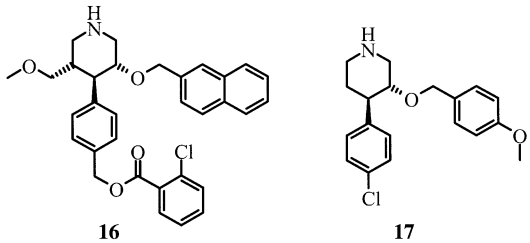

16 **17**

Scheme 5. Renin inhibitors.

and the potent ligand designed from it induce major conformational changes in the renin active site. Interestingly, these changes had not been observed previously, during a decade of X-ray crystallographic study, with peptidic ligands. These observations represent a new starting point for drug design programs. This is clearly not the end of the renin story, and it will be fascinating to see how modern discovery paradigms deal with this old target.

Structure-based design also contributed to the discovery of the carbonic anhydrase II (CA-II) inhibitor dorzolamide (**18**, Scheme 6), the first topical treatment for glaucoma.[54,55] Based on structural information, the methyl group was introduced into the thienothiopyran ring system, which stabilizes the alkylamino substituent in what would otherwise be the less favorable pseudo-axial conformation. The 4-alkylamino substituent induces a conformational change in the catalytically important residue His 64 causing it to occupy a position that is not observed for ligands bearing an N

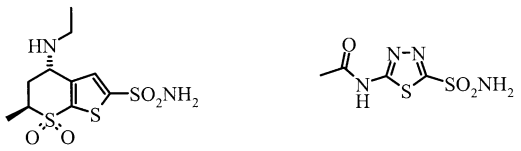

18 19

Scheme 6. Compounds for the treatment of glaucoma.

substituent smaller than ethyl. Introduction and optimization of the alkylamino substituent also enabled the manipulation of lipophilicity and solubility, which are critical factors for ocular penetration and formulation of a topical agent. Oral sulfonamide diuretics such as acetazolamide (**19**, Scheme 6) were used to treat glaucoma some forty years before the introduction of the topical agent dorzolamide.[56] Inhibition of carbonic anhydrase systemically has a myriad of consequences, and this limits the utility of oral, nonselective inhibitors. A nonselective agent must be present at very high concentrations in the blood in order to saturate carbonic anhydrase I, which is expressed at high levels in red blood cells. Only then can an efficacious level of the free drug be achieved, which results in inhibition of CA-II in the eye. With dorzolamide, because of the high local concentrations that can be achieved by topical treatment, and its selectivity for CA-II, an efficacious local concentration can be achieved at a 200-fold lower plasma concentration than would be required from an oral dose of acetazolamide. Carbonic anhydrase binding to red blood cells and its selectivity for CA-II totally dominates the pharmacokinetics of dorzolamide; its $t_{1/2}$ for elimination is approximately 120 days.

As might be anticipated, for topical agents the differences between a ligand and a drug are somewhat less. The pharmacodymanic and pharmacokinetic properties of dorzolamide are totally dominated by its affinity and selectivity for CA-II. In this sense, its properties as a ligand for its receptor have largely determined its success as a drug. This is not typical of drug discovery programs, however, since they are more frequently aimed at therapy through oral administration. More recently, structure-based design has been employed in the discovery of several agents that are now nearing market. For instance inhibitors of human nonpancreatic secretory phospholipase A2 (hnps-PLA2) have been obtained starting from the screening hit **20** (Scheme 7). Large movements of side chains were necessary to accommodate these inhibitors, and the movements would have been difficult to predict from the native structure.[57] The structures of a sequence of increasingly potent inhibitors such as **21** complexed with hnps-PLA2 were determined by X-ray analysis, and overall a 1000-fold improvement in potency in vitro was obtained. The study has resulted in LY315920 (**22**, Scheme 7), which is undergoing phase II clinical evaluation in inflammatory disease.[58] It will be interesting to see if this ligand proves to be an effective drug.

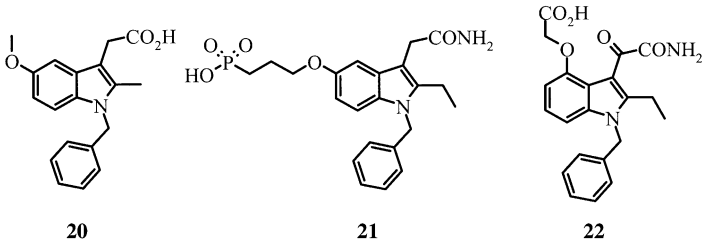

20 21 22

Scheme 7. Potential inhibitors of hnps-PLA2.

These examples illustrate the distinction between ligands and drugs. As these areas are relatively mature, the successes and difficulties can be viewed in the context of the whole journey from the initial concept to a drug in the clinic. The HIV protease, neuraminidase, and renin case studies are instructive when viewed in the light of the current understanding of druglike properties. The use of protein structural information in ligand optimization often leads to the maintenance and incorporation of polar interactions while the lipophilic contacts are increased in order to increase potency. However, the combination of these two strategies may not result in compounds with good druglike properties. The use of protein structural information in conjunction with in vitro potency determination may tempt medicinal chemists into designing ligands that are not drugs. High potency is not necessarily the most important requirement for a drug. The importance of ADME properties as well as potency is now recognized in most drug discovery programs. In order to be effective, the concentration of free drug must be maintained at a level at which the binding site on the target protein is significantly occupied throughout the dosing interval. This is a function of dose, clearance, plasma protein binding, intrinsic potency, volume of distribution, and dosing interval. Furthermore, an acceptable margin is required between the maximum concentration achieved at a therapeutic dose and the concentration that produces toxic side effects. The drug's pharmacodynamics and pharmacokinetics must be such that it meets these requirements at the desired dosing frequency.

Limiting the size, charge, and lipophilicity of a ligand in order to fulfill ADME requirements can limit the number of interactions made between the ligand and the residues composing the binding pocket. This limits the affinity that can be derived from interactions at the ligand–protein interface. This problem can be particularly acute where the ligand occupies a large binding site and mimics a large natural substrate, as is the case with many peptidases. The problem can sometimes be solved by using small ligands, which induce structural changes in the protein to fit the ligand. Greater affinity is obtained from a small ligand when it intercepts or induces a conformation of the protein, which produces a complex of lower total free energy. This is often the result of the ligand making favorable hydrophobic interactions with residues made available as a consequence of inherent conformational mobility of the protein.

3. Limitations in the Use of X-ray Data

A number of common and implicit assumptions are made by chemists who use protein structural data during structure-based design. These need to be highlighted, since they are often overlooked or even forgotten. First, we briefly define basic crystallography

terms, which aid in the interpretation of X-ray crystal structures. Then we discuss possible pitfalls and caveats in the structure determination, which are important for users of such structures.

3.1. Basic Crystallography Terms

In a crystallographic (X-ray diffraction) experiment, the raw data consists of the positions and intensities of the reflections as measured in the diffraction pattern of the crystal. From these intensities, the structure-factor amplitudes can be calculated (roughly as the square root of the intensities). Once the phases of the structure factors are also known (i.e., once the "phase problem" has been solved), Fourier transformation of the structure factors provides a map, which is a three-dimensional matrix of numbers that represent the local electron density.[59] Where there are many electrons (and, hence, heavier atoms) the density is higher than in places where (on average) there are few electrons. It is now the task of the crystallographer to interpret the electron density in terms of a discrete atomic model.[60] This is typically an iterative process, in which the crystallographer (or in favorable cases even a computer program) builds a part of the model and then refines this. The refinement program will make small changes to the model by adjusting parameters such as the atomic coordinates, which improve the ability of the model to explain the experimental data. Simultaneously, geometric and other restraints and constraints are enforced onto the model to ensure that it is chemically reasonable. With an improved model, new maps can be calculated that may reveal further details, for example, previously missing or uninterpretable density for loops, ligand, solvent molecules, etc. The crystallographer can then add these. Simultaneously, the crystallographer should be on the lookout for possible errors in the current model and correct them if possible.[61]

Besides coordinates, atoms in the model typically have a "temperature factor" (also known as B factors or atomic displacement parameters) to model the effects of static and dynamic disorder in the crystal. Except at high resolution (typically, better than ~1.5 Å), where there are sufficient reflections to warrant refinement of anisotropic temperature factors (requiring six parameters per atom), temperature factors are usually constrained to be isotropic (requiring only one parameter per atom). The isotropic temperature factor of an atom is related to the atom's mean-square displacement. In most cases temperature factors provide a useful relative indication of the reliability of different parts of the model. If they are high, for example, for a lysine side chain, this usually means that little or no electron density was observed for the atoms in that side chain, and that the coordinates are therefore less reliable.

Figure 1 shows the atomic coordinate records of a crystallographically determined structure stored in the Protein Data Bank (PDB).[62] Figure 1a gives an example of crucial information in the REMARK records of PDB entries. Inspection of these notes and of a validation report (e.g., the WHAT IF report on the PDBREPORT web site or the PROCHECK report on the PDBsum web site) is highly recommended. In this case, the structure of crambin has been determined (PDB entry 1EJG). Crambin exists in two isoforms that differ in two residues (either Pro22/Leu25 or Ser22/Ile25), and both forms were present in the crystal. The two sequence heterogeneities have been modeled as alternative conformations for residues 22 and 25, but due to format restrictions, only one sequence is recorded in the sequence records.

Figure 1b shows a fragment of a PDB file from the same entry. The basic information about the atoms in the model is listed on "cards" (records, lines). These begin with ATOM for protein or nucleic acid components or HETATM for entities that are ligands, ions, metals, and solvent molecules. The second item on each line is simply a sequential index number of that atom. In the first line atom 136 is the amide nitrogen atom (N) of the valine (VAL) residue A8. "A" is the chain name, "8" the residue number. The "A" before the residue symbol "VAL" signifies that this atom is statically disordered. This means that this atom is observed in more than one location in the electron density, and the various instances are labeled "A", "B", "C", etc. Indeed, the third line in the figure contains the alternative location "B" of this atom. The three real numbers that follow the residue number—"6.382, 2.222, 13.070"—are the Cartesian coordinates (x, y, and z) of the atom in orthogonal Å. The fourth number is the occupancy of the position. This is a number between zero and one, which indicates the fraction of the amide nitrogen atom of valine A8 that occurs in this location. Here, the first conformation has been given an occupancy is 0.55, and line 3 shows that the alternative conformation B accounts for the remaining 0.45. Note that quite a few programs that read and process PDB files ignore alternative conformations completely. When the occupancy of ligands and solvent molecules is refined or set to a number less than one, this implies that they occupy the position in only a fraction of the molecules in the crystal, or for only a fraction of the time, or a combination of both. The fifth number, 1.92 in line 1, is the value of the isotropic temperature factor (B factor). Line 2 reveals that this atom has been modeled anisotropically, (this involves six parameters per atom which are listed on the ANISOU card), but the isotropic equivalent value is always listed as the fifth real number of the ATOM (or HETATM) card. At the end of each card the atomic symbol of the chemical element of the atom is listed, since this cannot always be deduced unambiguously from the atom's name.

An important parameter in crystallographic studies is the resolution of the data, which is expressed in Å, where lower numbers signify higher resolution. The higher the resolution, the more experimental data, and the more reliable (in terms of accuracy and precision) one may expect the resulting model to be. At high resolution (<1.5 Å) the model is probably more than 95% a consequence of the observed data.[63] However, at lower resolution (>2.5 Å), the modeling of details in protein structures is much more subjective than is widely appreciated.[64] This can be understood by calculating typical data-to-parameter ratios, that is, the ratio of the number of experimental observations and the number of adjustable parameters (atomic coordinates, parameters asso-

a)

```
HEADER    PLANT PROTEIN                                 02-MAR-00   1EJG
TITLE     CRAMBIN AT ULTRA-HIGH RESOLUTION: VALENCE ELECTRON DENSITY.
...
REMARK 999 PRO/SER22:LEU/ILE25 ISOFORMS ARE MODELLED
REMARK 999 AS ALTERNATE CONFORMERS IN COORDINATE RECORDS.
REMARK 999 BECAUSE OF FORMAT RESTRICTIONS, ONLY PRO22/LEU25
REMARK 999 ISOFORM IS REPRESENTED IN THE SEQUENCE RECORDS.
```

b)

```
ATOM    136  N  AVAL A   8       6.382   2.222  13.070  0.55  1.92           N
ANISOU  136  N  AVAL A   8      421    149    160     33    -23    -35       N
ATOM    137  N  BVAL A   8       6.695   2.072  13.037  0.45  1.88           N
ATOM    138  CA AVAL A   8       5.099   2.259  12.380  0.55  2.32           C
ANISOU  138  CA AVAL A   8      397    258    224     16    -22   -120       C
ATOM    139  CA BVAL A   8       5.471   2.048  12.164  0.45  1.94           C
ATOM    140  C   VAL A   8       5.208   3.386  11.373  1.00  2.63           C
ANISOU  140  C   VAL A   8      380    402    213     71    -42   -209       C
ATOM    141  O   VAL A   8       4.712   3.302  10.238  1.00  2.67           O
ANISOU  141  O   VAL A   8      378    434    200     39    -31   -178       O
ATOM    142  CB AVAL A   8       3.944   2.394  13.375  0.55  3.36           C
ANISOU  142  CB AVAL A   8      376    635    262    186      4   -244       C
ATOM    143  CB BVAL A   8       4.263   1.630  13.035  0.45  3.05           C
ATOM    144  CG1AVAL A   8       2.629   2.981  12.701  0.55  4.22           C
ANISOU  144  CG1AVAL A   8      326    856    420    159     34   -159       C
ATOM    145  CG1BVAL A   8       3.580   2.930  13.664  0.45  3.89           C
ATOM    146  CG2AVAL A   8       3.635   1.036  13.955  0.55  4.82           C
ANISOU  146  CG2AVAL A   8      771    684    376    230    -61   -385       C
ATOM    147  CG2BVAL A   8       3.136   1.077  12.028  0.45  4.17           C
ATOM    148  H  AVAL A   8       6.374   2.231  14.084  0.55  2.27           H
ATOM    149  H  BVAL A   8       6.648   2.059  14.045  0.45  5.91           H
...
END
```

Figure 1. a) An example of crucial information presented on REMARK records in PDB entries. b) Fragment of a PDB file from the same entry. The basic information about the atoms in the model is listed on "cards" (records, lines). For a complete description please refer to the text.

ciated with the temperature factors, and occupancies amongst others) in the model. For an average protein structure at a resolution of 2 Å, this ratio is slightly greater than two, but at ~2.7 Å it becomes less than unity. Whereas gross errors in the structure are unlikely to persist to the publication stage if the resolution is high, once the resolution becomes >2 Å, the balance shifts. Some published protein models appear to have been more determined by the crystallographer's imagination than by any experimental data.[63] In fact, in the 1980s the first reports of some of the "hottest" protein crystal structures, some of which were also prime drug targets, contained extremely serious errors.[65] Examples included HIV-1 protease, photoactive yellow protein, the small subunit of RuBisCO, D-Ala-D-Ala peptidase, ferredoxin, metallothionein, gene V binding protein, and the GTP-binding domain of Ha-ras p21.

Recently, the structure of a complex between botulinum neurotoxin type B protease and the inhibitor BABIM was published,[66] and the structure and experimental data were deposited in the PDB (entry 1FQH). However, subsequent critical analysis of the electron-density maps revealed that these did not support the placement of the inhibitor as stated in the earlier paper, and the structural conclusions based on it were withdrawn by the authors.[67]

Another trap to be aware of (and one that many crystallographers have fallen into) is the derivation of "high-resolution information" from low-resolution models. For instance, in a typical 3-Å structure the uncertainty in the position of the individual atoms can easily be 0.5 Å or more. Nevertheless, many such models have been described where hydrogen-bonding distances are listed with a precision (note: not accuracy!) of 0.01 Å (probably because the program that generated these distances used that particular precision) and solvent-accessible surface areas with a precision of 1 Å^2.

The ability of the model to explain the experimental data is usually assessed by means of the (conventional) *R*-value, which is defined in Equation (1).

$$R = \left(\sum \| F_{\mathrm{obs}} | - \mathrm{scale}\, | F_{\mathrm{calcd}} \| \right) / \left(\sum | F_{\mathrm{obs}} | \right) \qquad (1)$$

Here, F_{obsd} are the experimental structure-factor amplitudes, F_{calcd} are the structure-factor amplitudes calculated from the model, and the sums extend over all observed reflections. However, when more and more parameters are introduced into the model, the *R*-value can be made almost arbitrarily small (this is called "over-fitting the data"). In 1992 Brünger[68] introduced the concept of cross-validation in

crystallographic refinement, and with it the free *R*-value (*R*free), whose definition is identical to that of the conventional *R*-value, except that the free *R*-value is calculated for a small subset of reflections that is never used in the refinement of the model. The free *R*-value therefore measures how well the model predicts experimental observations that are not used to fit the model. Until a few years ago a conventional *R*-value below 0.25 was generally considered a sign that a model was essentially correct. While this is probably true at high resolution, it was subsequently shown for several intentionally mistraced models that these could be refined to deceptively low conventional *R*-values.[65,69] Brünger suggests a threshold value of 0.40 for the free *R*-value, that is, models with free *R*-values greater than 0.40 should be treated with caution.[70,71] Since the difference between the conventional and free *R*-value is partly a measure of the extent to which the model overfits the data (i.e., some aspects of the model improve the conventional but not the free *R*-value and are therefore likely to fit noise rather than signal in the data), this difference (*R*free $-$ *R*) should be small for the final model, ideally < 0.05.

3.2. Uncertainty in the Identity or Location of Protein or Ligand Atoms

It is often forgotten that an X-ray crystal structure is one crystallographer's subjective interpretation of an observed electron-density map expressed in terms of an atomic model. This structure is treated by chemists undertaking structure-based design as if it were at perfect resolution, independent of the resolution at which the structure was actually determined and ignoring the interpolations, assumptions, biases, and sometimes mistakes incorporated by the crystallographer.

Uncertainties can involve the identity of important atoms like those in the binding pocket. For instance at a resolution typical for macromolecules (~2 Å) the relative positions of the δN and δO atoms of asparagine and γN and γO atoms of glutamine side chains cannot usually be determined directly from the electron density since they are isoelectronic. The decision as to which density feature should be assigned to N and O should be based on inspection of the local hydrogen-bonding networks. However, these decisions may have to be made before solvent molecules have been added to the model and hence be based on incomplete hydrogen-bonding networks. Moreover, in low-resolution structures many of the solvent entities are not resolved in the electron density and can therefore not be modeled, thereby further complicating the analysis. A careful crystallographer will verify the assignment in the final model, but in general the users of the model should treat the final assignment with caution. This is also borne out by large-scale analysis of the hydrogen-bonding patterns involving histidine, glutamine, and asparagine residues with the program WHAT IF,[72] as listed on the PDBREPORT web site.[73] This analysis suggests that as many as one in six of all histidine, asparagine, and glutamine residues in the PDB may have been modeled in a "flipped" orientation.

Uncertainties can also occur at the level of whole residues. This is the case for flexible residues, which often diffract so weakly that no clear electron density is observed for them. This is quite common for the side chains of surface residues, but may also be found in some active sites, particularly with the flexible side chains of lysine and glutamate. Analysis of real-space density fits[74] shows that most poorly defined residues are, in order of improving average fit to the density, Lys < Glu < Arg, Gln < Asp, Asn. The crystallographer knows they are present from the amino-acid sequence, and so they are incorporated into the structure in a conformation commonly observed for that residue in databases of high-resolution structures. The final conformation of the side chain, as viewed by the chemist, can be the product of intelligent guesswork and the van der Waals term in the refinement program's force field, rather than experimentally observed electron density. It is also quite common for whole sections of the protein to give little or no observable electron density. Sometimes these parts are mobile loops and these can have great functional significance also, by virtue of this greater mobility.[75] In other cases, entire domains may be invisible in the electron-density maps.

Similar ambiguities apply when the bound ligand is considered. For instance, the position of pyridine nitrogen atom cannot usually be determined from the electron density alone. This fact will introduce uncertainty into many crystal structures containing a molecule with an asymmetrically substituted pyridine. For instance, during the study of benzo[*b*]thiophene inhibitors of thrombin, compound **23** was complexed and a structure built based on the measured

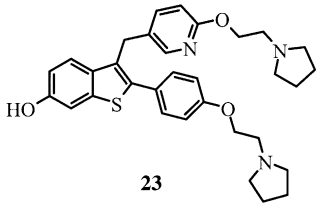

23

electron density. The C3 pyridyl ring was oriented arbitrarily so that the nitrogen atom resides in the more hydrophilic of the two possible environments. This is a reasonable assumption, but not the result of direct experimental observation and so is still uncertain.

An example of how ambiguous X-ray crystallographic data can be when the exact chemical composition of a ligand or residue is not known was encountered recently. The exact identity of the twenty-second genetically encoded amino acid pyrrolysine **24**,[76] present in *Methanosarcina barkeri* monomethylamine methyltransferase (MtmB), is still unknown even though a 1.55-Å resolution structure of the protein is available. The X substituent is a methyl, ammonium, or hydroxy group.

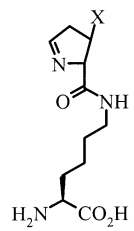

24

On the other hand, sometimes (careful) crystallography can reveal cases of mistaken identity. For example, when the structure of cellular retinoic-acid-binding protein type 2 (CRABP2) in complex with a synthetic retinoid was solved, it was assumed that the ligand

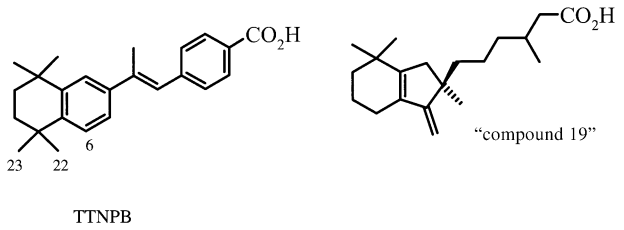

Scheme 8. Postulated and actual CRABP2 ligand.

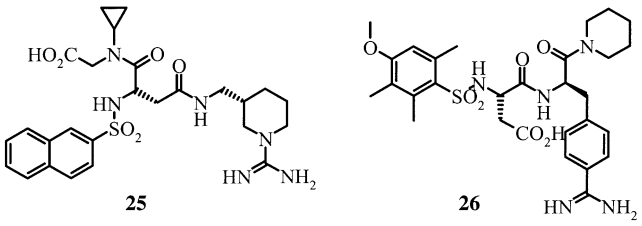

Scheme 9. Thrombin inhibitors napsagatran (**25**) and CRC220 (**26**).

was TTNPB (Scheme 8).[77] The ligand was built and fitted to the density, but the maps stubbornly suggested that there was something wrong. The density failed to cover the whole ligand, and features in the map suggested that there ought to be a carbon-like atom at a distance of ~1.5 Å from C6, and that atoms C22 and C23 should be removed from the model. After double-checking the identity of the ligand with the chemists, the crystallographers found that the ligand that was actually complexed to the protein was "compound 19" (Scheme 8). The structure of this ligand made perfect sense in terms of the density (Figure 2), and the refinement of the structure could be completed successfully. However, had the resolution been 3 Å instead of 2.2 Å, the error might well have gone undetected.

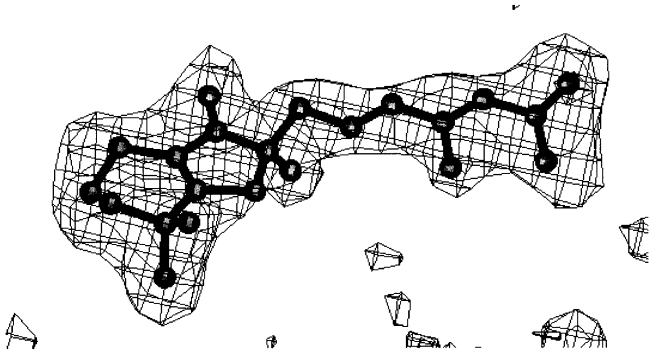

Figure 2. Electron density for and structure of "compound 19" in complex with CRABP2.

Since the presence of hydrogen atoms is inferred rather than observed, the tautomeric state of histidine or of bound ligands containing tautomeric groups cannot be determined directly. The latter problem is rather common in studies involving acid isosteres. Similarly, the state of ionization of the ligand or protein cannot be observed. It is usually assumed that the charged state of the protein is known. However, the pK_a values of common acidic or basic side chains can differ drastically from their normal values as measured in water, when they are located in the microenvironment of a protein active site.[78] Even when the protonation states of key active-site residues and the ligand are known, these may change upon complexation. Enthalpies of complexation measured by isothermal titration calorimetry, in aqueous buffers with different enthalpies of ionization, established that the Roche thrombin inhibitor napsagatran (**25**, Scheme 9) binds to thrombin incorporating an additional proton.[79] An inhibitor with a similar structure, CRC220 (**26**), from Behring binds to thrombin without an additional proton. This difference in ionization, upon binding to the protein, was supported by different orientations of the ligands when the structures of the complexes with thrombin were determined by X-ray crystallography.

3.3. Effect of Crystallization Conditions

The conditions required to crystallize a protein or to optimize diffraction may not be the same as those employed in the biological assay. This may affect the reliability of rationalization and prediction of structure–activity relations (SAR) from sequential protein–ligand complexes. The influence of crystallization conditions is often unknown or not considered, but numerous examples highlight its importance. An unusual cubic form of trypsin was observed when it was complexed with compound **27** at pH 7.[80] The same ligand–protein complex crystallized at pH 8 shows a different ligand

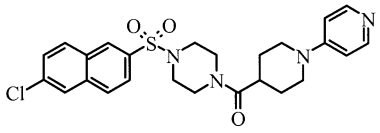

27

conformation, active-site conformation, and crystal morphology. Normally the pH during protein crystallization has no effect upon the formation of various crystal forms, but in the case of **27** the pH affects the protonation state of the ligand and thereby alters its binding mode, which in turn precludes the normally observed packing of the protein.

The terminal methylpiperazine ring of Abbott inhibitor A-70450 (**28**) was found to exist in a chair conformation in the crystal structure of secreted aspartic protease 2X crystallized at pH 4.5.[81] But in a subsequent study the methylpiperazine group was observed to assume a boat conformation when the complex was crystallized at pH 6.5.[82]

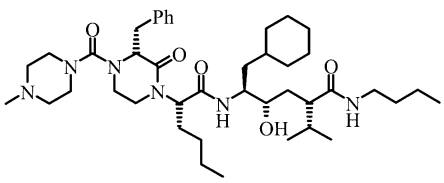

28

The recently identified genetically encoded amino acid pyrrolysine adopts two conformations in MtmB. The occupancies of the two conformations depend upon whether the precipitating salt was sodium chloride or ammonium sulfate.[76] When ammonium sulfate is used as the precipitating agent, additional density adjacent to C2 of the ring suggests the addition of ammonia from the buffer to the imine of pyrrolysine. The change in occupancy of the two conformations appears to be controlled by new hydrogen bonds formed between this nitrogen atom and Glu259 and Gln333.

Two crystal forms of human pancreatic α-amylase were also observed at different pH values. The flexible loop, which is typical of mammalian α-amylases, was shown to exist in two conformations, which suggests that loop closure is pH sensitive.[83] Likewise, pH-sensitive changes in conformation have been observed for glycinamide ribonucleotide transformylase,[84] *Aspergillus* pectin lyase A,[85] glutathione synthetase,[86] influenza matrix protein M1[87] and ribonuclease A.[88]

3.4. Identification and Location of Water Molecules

Identification of water molecules in the electron-density maps can be a problem. Water, sodium ion, and ammonium ion—common constituents in crystallization media—cannot always be distinguished based on their density alone, because they are isoelectronic. The local environment must be taken into account in order to decide how a solvent feature in the electron-density map is best interpreted. Such issues are easily missed, especially by less experienced crystallographers.

The location of water molecules can also be problematic. Unless the resolution is high, the presence or absence of water molecules cannot be determined with certainty, and it becomes a subjective matter whether a feature in the density should be ignored as noise or modeled as a water molecule. However, uncritical addition of solvent molecules (each of which introduces four adjustable parameters, x, y, and z coordinates and an isotropic temperature factor, into the model) provides the crystallographer with an excellent means of absorbing problems in both the experimental data and the atomic model.[63,69] Addition of water molecules is then simply used to artificially reduce the differences between observed and calculated structure-factor amplitudes.

When crystallographers determine the same structure at similar resolution, their water structures are bound to reveal many discrepancies. For example, the structure of transforming growth factor-β2 was determined by two independent laboratories at similar resolutions, 1.8 Å (1TGI) and 1.95 Å (1TFG).[89] There are 58 water molecules in 1TGI with an average temperature factor of 31.8 Å^2 and 84 water molecules in 1TFG with an average temperature factor of 43.3 Å^2. In 1TFG the 54 water molecules common also to 1TGI have much lower temperature factors (average 34 Å^2) than the 30 extra water molecules (average 60 Å^2), which suggests that the latter have a much lower level of reliability. The structure of human interleukin 1β was determined independently in four different laboratories at similar resolution.[90] The four models contained between 83 and 168 water molecules, but a mere 29 of these were in common to all four models. Interestingly, although all 29 belong to the first layer of solvation, not all of them are buried. In a final example the structure of poplar leaf plastocyanin was subjected to two separate refinements by independent laboratories who used the same set of synchrotron X-ray data at 1.6 Å.[91] The two groups used two different refinement protocols and agreed not to communicate until each was convinced that their refinement calculations were complete. The structures contained 171 and 189 water molecules, respectively, but only 159 water molecules were common to both structures within 1 Å. While it can be a matter of subjectivity to decide whether the electron density supports the presence of a water molecule at a particular location, a water molecule that does not form a single hydrogen bond to any other atom is almost certainly an artefact. Statistics from the protein verification tool WHAT IF,[72] found at the PDBREPORT web site[73] identify 99 793 water molecules in 10 857 structures deposited in the PDB that have no hydrogen bonds to any other atom in the structure (September 2002).

It may simply be worth remembering that at the resolution usually encountered in structures in pharmaceutical discovery projects, the electron density for water molecules that are not well ordered is often difficult to distinguish from noise. The importance of water in binding energetics and kinetics should not be overlooked (although it sometimes is). Water is the "third party" in the ligand–receptor interaction.[92] Depending on the hydrogen-bonding environment of influential water molecules, it may be energetically favorable for a ligand to displace the water molecule, form a hydrogen bond to it, or not to interact with it. With uncertainties over which water molecules are displaced, and which are not displaced from the active site upon ligand binding, water molecules are often completely removed in virtual screening campaigns. This oversimplification may affect the accuracy of docking and scoring.

4. PDB Files Used in Docking and Scoring Studies

An important criterion in the choice of protein–ligand complexes used to validate docking and scoring programs is the resolution of the structure. But even at high resolution the ligand may still not be well defined, as recently highlighted by Boström.[93] The structure in PDB entry 1PME was determined to a resolution of 2.0 Å, however the planar methanesulfonyl group present in the ligand is chemically unlikely. Similarly, the 3-phenylpropylamine ligand in structure 1TNK, which was determined to a resolution of 1.8 Å, contains a tetrahedral aromatic carbon atom bound to the propylamine chain. Visual inspection would reject these structures, so it is surprising that 1TNK also features in the validation set for Flex-X. One lesson is that whereas high-quality dictionaries of acceptable bond lengths, angles, and torsions are available for amino and nucleic acids in model refinement, the same is not true for complexed ligands. This is because of the huge diversity of small molecules compared to amino and nucleic acids. The Hetero-Compound Information Centre, Uppsala, (HIC-Up[94]) has made available ready-made dictionaries for

commonly used crystallographic protein modeling software (CNS, X-PLOR, TNT, and O) as an aid to crystallographers.[95] A similar service is provided by the PRODRG server.[96] Also accessible through the HIC-Up site is a basic validation tool, HETZE, which checks the PDB file of a ligand for acceptable ranges of bond lengths, angles, and torsions.

Sometimes complexes are selected as docking targets, even though the experimental evidence is not sufficiently strong for an unequivocal decision on the ligand orientation. For instance, the position of the carboxylate group of oleic acid in a mutant rat intestinal fatty acid binding protein (IFABP) was ambiguous when the electron density was examined.[97] Indeed, the crystallographers report three positions for the carboxylate group in the deposited PDB file (1ICN), with occupancies of approximately 0.3 for each. Surprisingly, this complex, despite its uncertain structure, was selected as a validation structure when Flex-X was tested with the DOCKSCORE scoring function[14] and GOLD. In hindsight then, it may not be surprising that Flex-X and GOLD failed to reproduce any of the observed conformations of oleic acid. Flex-X calculated that the highest scoring conformation for oleic acid is rotated 180° in the active site relative to the orientation reported in the PDB file. It was suggested that the original crystallographic assignment for the position of oleic acid was incorrect and that the orientation predicted by Flex-X was in better agreement with the electron density. However, limited rerefinement of the model from which the carboxylate groups were removed, against the original experimental data, but with current methodology reveals no clear density for the carboxylate group at either end of the ligand (Figure 3a–c). Normally, in this family of proteins, two arginine residues are involved in binding the carboxylate group of the ligand. Wild-type IFABP is already the odd one out in the family, since one of the arginine residues is involved in a salt bridge with an aspartate residue. In the present structure the remaining arginine was mutated to glutamine, and therefore it seems unlikely that there is any driving force to cajole the carboxylate group of the fatty acid into entering the interior cavity of the protein. Instead, it seems more likely that the carboxylate group sticks out into the solvent. Such a binding mode has been observed in the crystal structure of another fatty-acid-binding protein.[98] Moreover, subsequent NMR experiments by Jackoby et al. on the mutant complex[99] showed that the carboxylate group of the ligand is exposed to solvent.

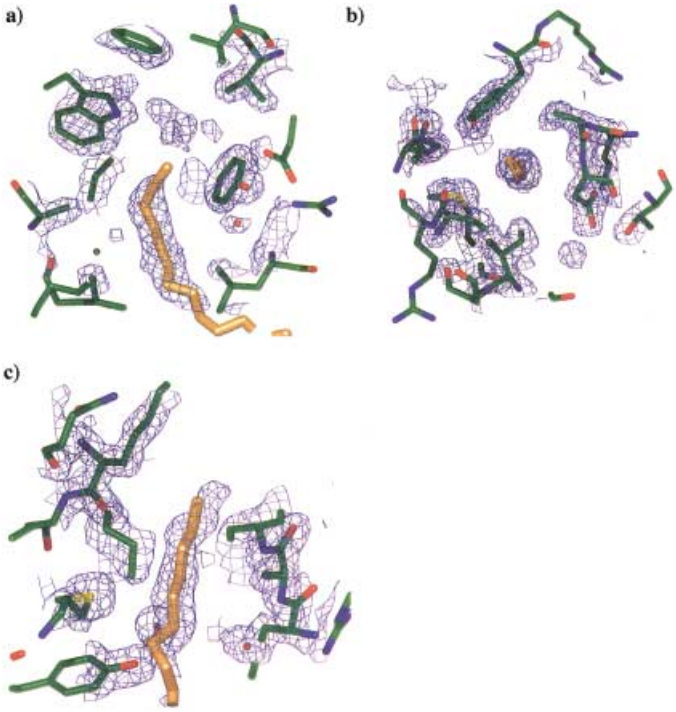

Figure 3. a) Oleic acid complexed to an IFABP mutant after limited refinement (data not shown). Although some extraneous electron density (blue mesh) is visible, it is neither possible nor sensible to assign it to the ligand's carboxylate moiety. b) Electron density near the opposite end of the ligand. It is clear that there is no density to support either the presence of the carboxylate group or any contacts with main-chain amides. This view is from outside the protein into the ligand-binding cavity. c) Electron density at the other end of the ligand model shows that the ligand points into the solvent. Most likely the carboxylate group is located here, but due to disorder there is no density for it.

Recently, the Cambridge Crystallographic Data Centre and Astex Technology Ltd have produced a "clean" list of protein–ligand complexes for validating docking and scoring algorithmns.[100] All entries in the "clean" list have been checked manually to exclude protein–ligand complexes that contain factual or structural errors in the PDB file, unlikely ligand conformations, and severe protein–ligand clashes, as well as those complexes in which the crystallographically related protein chains influence the binding geometry.

5. Assessing the Validity of Structure Models

In view of the uncertainties concerning the validity of X-ray structures deposited in the PDB, about which even experts disagree, the average user does well to proceed with caution. The degree of confidence in the position of a particular atom or residue can be assessed by using the temperature factors, occupancies, and occasionally remarks, all of which are deposited with the atomic coordinates. If the structure factors are also deposited, electron-density maps can be calculated and superimposed on the structure. Examination of the structure together with the electron-density map is highly recommended.[101] This enables users of the refined model to assess the quality of the fit of the model to the density (data). Issues that can be addressed include the overall reliability of the model, together with the position, orientation, conformation, and geometry of specific residues and ligands. This level of detailed visualization is generally only available in specialist crystallographic modeling tools such as O, but the program DEEP VIEW, which is freely available on the internet allows full visualization of PDB files together with electron-density maps.[102] It is not always possible to inspect the density, since this requires that the structure factor data have been deposited with the PDB by the crystallographer. Although most journals now have strict deposition policies, a recent

survey found that for only ~30% of all crystal structures in the PDB could electron-density maps be calculated.[103] Interestingly, it appears that more structure factors are deposited for structures with low than for those with high free *R*-values. This curious observation suggests that the worse the model is, the less likely it is that the crystallographer will deposit the experimental data that the structure is supposed to explain. Jones and co-workers have developed the Uppsala Electron Density Server[104] to facilitate objective assessment of the quality of the fit of the model to the electron density of any PDB entry for which structure factors are available.[74]

Figure 4. Active sites of the oxidized and reduced forms of a nitrite reductase. The electron density associated with Asn98 (brown mesh) is only partly filled, consistent with multiple conformations for this residue. Similarly the poor fit around the bound nitrite group indicates disorder (reproduced from ref. [107] with permission).

Before expending considerable resources on the exploitation of a protein–ligand structure, medicinal chemists and protein modelers would do well to assess the overall reliability of the model. An introductory tutorial for nonexperts is available on the internet.[63,105] Subsequently, researchers should assess the reliability of any crucial residues, water molecules, and bound ligands, either by interacting directly with the crystallographer who determined the structure or by reading the literature. Scrutiny of the REMARK records in the PDB entry and inspection of the temperature factors and occupancies is recommended. Treating a PDB entry as a simple array of atom coordinates at perfect resolution is a gross oversimplification and can easily lead to false assumptions concerning the model.

Two examples, from many which might be chosen, illustrate the point. Two molecules of 1-deoxynojirimycin were observed bound in the active site of glucoamylase from *Aspergillus awamori* varX100 in a structure determined at 2.4-Å resolution.[106] One of the ligands shows strong electron density, whereas the second molecule appears to occupy the second binding site only partially. The authors comment that the "secondary binding site for 1-deoxynorjirimycin should be regarded with caution and may not reflect the true binding of the substrate to the second subsite". With such uncertainty a medicinal chemist might expect that the second site would be left empty in the deposited coordinate file. In fact, the PDB entry contains both 1-deoxynojirimycin molecules, albeit that the second one is flagged in a way that makes perfect sense to crystallographers, but which inexpert users of the structure files are almost bound to overlook. The choice of whether to include partially occupied binding sites or multiple side chain conformations is largely arbitrary. For instance, disorder was observed for both the nitrite ligand and an active site asparagine residue in the mutant Asp98Asn form of *Alcaligenes faecalis* S-6 nitrite reductase,[107] in a structure determined at 2.0-Å resolution (Figure 4). Although the electron density clearly shows two binding conformations for Asn98, this time only one conformation is reported in the PDB entry.

Confidence in a model can be gained when multiple, independently determined protein–ligand complexes are available, at very good resolution, and when the electron-density maps are inspected closely. Important factors can then be assessed such as the position of influential water molecules,[108] the degree of flexibility in residues neighboring the active site, and assumptions that may influence the success of structure-based design and docking studies.

Assumptions crystallographers make in modeling the electron density may appear minor when one considers the correctness of an entire ligand–protein structure. However, these assumptions can have a profound effect when the structure is used subsequently as the basis for a structure-based design project. While some of these problems are minimized at high resolution (< 1.5 Å), many structure-based design projects routinely rely on protein structures determined at significantly lower resolutions than this. The structure generated from the electron density may be good. In any one target or ligand series, protein flexibility may be unimportant. It is possible that sensible decisions about influential water molecules can be made. The binding site may be wholly contained within a single copy of the protein and therefore little influenced by other copies of the protein in the unit cell. Therefore there may be many situations in which current manual design and docking and scoring programs have utility. However, great care should be exercised and assumptions in the structure should be assessed continuously.

6. Automated Docking and Scoring

Successful structure-based design requires accurate and reliable docking algorithms and the ability to predict the affinity of the docked ligand for the target structure. Many of the standard packages have been reviewed recently (Table 1).[39] The most widely used programs at present are probably DOCK, Flex-X, and GOLD. GOLD is arguably the most rigorously validated docking algorithm presently avail-

able. It utilizes an algorithm that allows full ligand flexibility during docking, while protein flexibility is limited to very small movements in the protein active site, for instance rotation of OH groups to allow for optimal H-bonding. The GOLD web site includes some examples of successful docking, including that of a peptide ligand into actinidin and of GMP into ribonuclease T1. Its web site also provides access to overlays of all the docked ligands from the validation set with the deposited conformation taken from the PDB file.[109] Indeed one of its most attractive features is the rigorous and self-critical validation of the program.

The GOLD validation methodology is typical of docking and scoring evaluations. It is based on redocking calculations where the ligand is docked back into its own receptor pocket. This is not representative of the actual design process, however, where a single or at best a small number of protein structures are utilized to dock many ligands. The test is also somewhat artificial in that the protein conformation is predetermined, the approximate binding site indicated, and various assumptions made concerning the ionization state of individual residues. A recent survey of the success of redocking using the PROLEADS program has succinctly highlighted the deficiency of redocking as an objective way of assessing a new docking algorithm.[110] Six or more protein–ligand complexes were taken for a single target. Although PROLEADS was successful 76% of the time at redocking individual ligands into their own active sites, it was successful only 45% of the time in docking another ligand from the set to that same active site. Small, apparently insignificant, changes in the protein structure around the ligands are enough to adversely affect the chances of successful docking. The study was carried out for ligands of the proteins thrombin, thermolysin, and neuraminidase.

Successful ligand design also requires accurate scoring of a molecule's potency. Scoring allows the ranking of multiple docked conformations and/or the prediction of binding energy. Scoring of docked conformations is recognized as a major weakness in current algorithms. While it would be anticipated that scoring functions do rather well at predicting the potency of complexes that were used in the derivation/training set for that scoring function, the most objective assessment of performance is how well they predict new complexes. Three commonly used scoring methods are master equations, knowledge-based functions, and trainable functions.

Approaches based on master equations are implemented in a number of leading algorithms, of which the LUDI scoring function was the first and most widely imitated. The total binding energy is partitioned into contributions from hydrophobic, hydrogen-bonding, and charge interactions, corrections for suboptimal hydrogen-bond geometry, and the energetic cost of the degrees of freedom for bond rotation lost upon binding. The coefficients of the LUDI master equation SCORE1 were determined initially by regression analysis of the interactions observed by X-ray structure determination of 45 ligand–protein complexes together with the affinities of each ligand for its cognate receptor. These are in good agreement with independent assessments of the contributions to binding obtained from thermodynamic measurements. For instance, the contribution of hydrophobic interactions is scored at $0.17\ kJ\,A^{-2}\,mol^{-1}$, which is in good agreement with estimates of $0.12\ kJ\,A^{-2}\,mol^{-1}$ from solvent-partitioning measurements and detailed SAR studies.[111,112] The contributions of hydrogen bonds are scored at $4.7\ kJ\,mol^{-1}$ per hydrogen bond. This value is also in reasonable agreement with estimates of up to $6.3\ kJ\,mol^{-1}$ derived from detailed study of tyrosyl t-RNA synthase, a value of $2–6\ kJ\,mol^{-1}$ from physical-organic studies on vancomycin,[113] and SAR studies on sugars binding to glycogen phosphorylase.[114]

Knowledge-based approaches (SmoG,[15] DRUG-SCORE,[14] and PMF[115]) are currently receiving considerable interest. Knowledge-based potentials are derived from evaluations of close contacts between atoms in a large selection of protein–ligand complexes by means of statistical mechanics. Binding energy is represented as the sum of free energies of interatomic ligand–protein contacts, which are calculated from their frequencies of occurrence in the complexes. The knowledge-based approach implemented in SmoG2001 gave a root-mean-square error (RMSE) of 1.69 log units in predicting the potency of a test set of 77 complexes. The authors compared SmoG2001 with SCORE1 (LUDI) by using the same test set and found that SCORE1 (LUDI) gave an RMSE of 3.47 log units, which suggests that SmoG2001 is a considerable improvement upon SCORE1 in prediction.

One drawback of master-equation or knowledge-based approaches is that the relative contribution of different types of interactions to ligand affinity may change between families of active sites, because of differences in hydration or polarity within the active site.[116] However, the scoring function for VALIDATE can be trained on the series of interest in contrast to a generic scoring function.[117] A large number of ligand–protein complexes, covering a sufficient range of potencies, are required, since the approach is based on QSAR methods. Physicochemical descriptors are calculated for the ligand and the ligand–protein complex and are correlated against affinity in order to generate empirical predictive models. Thus, VALIDATE was trained by using 39 HIV-protease inhibitor complexes having a potency range of $pK_i = 6.4–11.4$.[118] This HIV-protease VALIDATE model was then used to predict the binding constants of 363 HIV-protease inhibitors reported in the literature. Actual versus predicted affinities for the validation set are given in Figure 5.

The current performance of scoring functions such as LUDI, SmoG2001, and VALIDATE in predicting potency is usually insufficient to be useful in optimizing leads. Here the aim is usually to convert a lead having 1–10 μM activity into a potential development candidate having 1–10 nM activity. This 100- to 1000-fold increase in potency appears to be within the random error of these scoring functions. However, this is not universally the case. One successful example where scoring was applied in lead optimization was in the design of peptidic HIV-protease inhibitors at Merck.[119] The scoring was calculated based on consideration of the electrostatic and steric interaction energies after energy minimization of the docked ligand (**22**) in the protein active site. Although the absolute prediction of potency depended upon which protein structure was used for the dockings, the correlation between

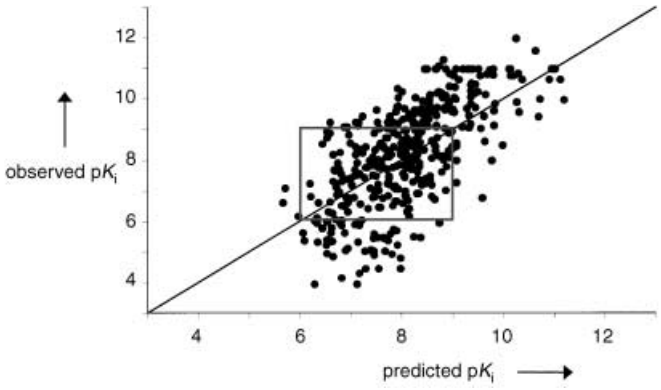

Figure 5. A plot of observed pK_i values versus values predicted by VALIDATE II for a test set of HIV-protease inhibitors not used to train VALIDATE II. The line of unity is displayed. The box indicates the 1000-fold potency range in which lead-optimization projects typically operate (reproduced from ref. [118] with permission).

predicted potency and actual potency was remarkably good, as were predictions on novel compounds, which were subsequently synthesized.

A further major assumption underlying the use of docking and scoring programs is that the receptor is not flexible, or at least that receptor flexibility is an infrequent occurrence. This assumption has been questioned recently, and a number of examples of induced fit and protein flexibility have been reviewed.[120] Indeed, induced fit appears common for drug-like compounds rather than being an infrequent occurrence.[121] The incorporation of protein flexibility into automated docking and scoring algorithms is presently an important focus. Several approaches are being taken to try to address this problem, with various degrees of rigor. These include the use of a "soft" scoring function, which allows some overlap between the ligand and the protein, protein-ensemble approaches in which the protein is represented as a composite of a number of different conformations, and constrained molecular dynamics simulations in explicit water.[122–124]

It is sometimes possible to overcome the uncertainties in the scoring functions by using them to design combinatorial arrays of putative ligands rather than individual compounds. For instance, Multiple Copy Simultaneous Search (MCSS) was used to identify subsites within the picornaviral capsid ligand-binding site.[125] This information was applied to the design of targeted libraries and hits obtained. Interestingly, because of induced fit, the position of one of the ligands was reproduced only when protein side chains were allowed to move. The authors comment that the advantage of libraries over individual compounds is that the scoring function for selecting ligands need not be highly accurate. The scoring function is required only to have enough information to guide and focus libraries. Even though small changes in protein structure do occur upon ligand binding, a combinatorial approach ensured that the appropriate ligands were synthesized anyway. Combinatorial chemistry and structure-based design were combined to provide a useful tool.

7. Convergence of Screening and Structure-Based Design

Many drug discovery programs demonstrate an important complementarity between HTS and structure-based design. HTS often yields many weak leads, and chemists make intuitive decisions about which leads to follow. Structural studies can dramatically influence the priority placed upon a particular hit.

Obtaining structural information on chemically diverse leads can reveal hitherto unsuspected mobility in active-site residues. These observations can provide new insights and opportunities for optimization. Combinatorial chemistry can be used to probe areas of the binding pocket in the search for new interactions. For instance, MMP3 inhibitors have been developed[126] by replacement of the N-methylacetamido group in **29** by phenyl (Scheme 10). This unexpected replacement was discovered by applying combinatorial chemistry and subsequently explained by X-ray crystallography. Structural information on the induced binding site prompted further rounds of design and evaluation, leading to replacement of the *p*-methoxyphenyl group by pyridyl (**30**).

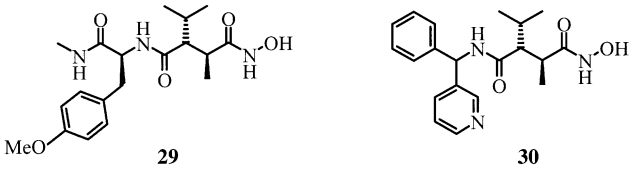

Scheme 10. MMP3 inhibitors.

The design criteria for an ideal HTS compound library have been shifting from mere diversity towards "druglike" properties and even further towards "leadlike" libraries[127,128] and compound collections. The lead optimization process tends to result in compounds with increased molecular weight and complexity,[129] and this has resulted in an intense search for methods to identify small leadlike templates. NMR spectroscopy and X-ray crystallography may be superior to HTS for identifying small ligands since low-molecular-weight ligands may not contain enough functionality to demonstrate significant inhibition at the concentrations typically used in HTS. The VERTEX SHAPES,[25] Fesik's SAR-by-NMR,[24] and high-throughput crystallography approaches,[26,27] are being utilized increasingly to find small binding motifs with activities in the mM-to μM-range that can be effective starting points. This strategy also allows for the rapid design of new hybrid structures. Surprising observations are often made concerning binding orientations of ligands and the mobility of binding site residues.

The additivity of substrate fragments in an enzyme–ligand binding site was demonstrated with thymidylate synthase complexed with fragments of deoxyuridine monophosphate, **31**–**35** (Scheme 11).[130] The complexes show considerable fidelity of binding orientation, which suggests a modular approach to ligand design by utilizing small molecular fragments. The advantage of NMR spectroscopic and crystallographic techniques is that fragments which bind in the

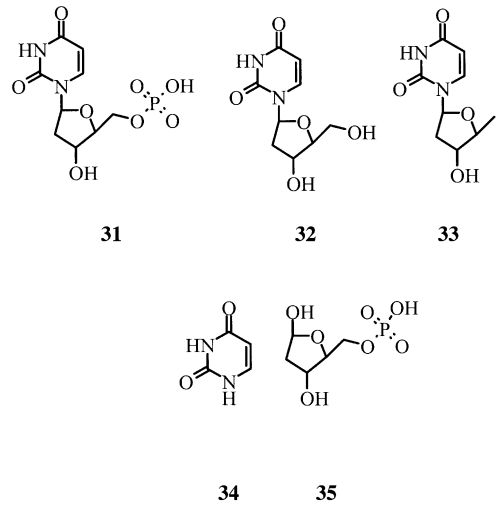

31 32 33 34 35

Scheme 11. Deoxyuridine monophosphate fragments.

millimolar range can be used and spatial information obtained. The disadvantages include expense, high dependence on solubility of the fragments, modest numbers of templates screened, and labor-intensive analysis. Typically protein crystals may not be tolerant of the high concentrations of compounds and DMSO used. 1D NMR techniques are typically used as a preselection tool. The elegance of these approaches has led to the setup of a number of small start-up companies offering the techniques as part of a collaborative effort. The assumption that a number of low-affinity templates can be combined to yield a molecule with an affinity greater than the sum of these components is implicit in these techniques. However the common practice of obtaining affinity with one subsection of a molecule and then addressing ADME requirements by adding further groups is fraught with difficulty. For drug design the requirement is often to achieve the required properties by using a limited number of atoms such that parts of the molecule address several property objectives simultaneously.

Some screening technologies like SAR-by-NMR or high-throughput crystallography have greater information content but more limited throughput than traditional HTS screens. Virtual and property-based screening methods can be used to address this when they are used to pick a subset of the total compound collection. Sometimes virtual screening and HTS campaigns are run in parallel. Pharmacia screened their 400000-compound corporate library against protein tyrosine phosphatase-1B in parallel with a virtual screen of 235000 commercially available compounds with DOCK3.5.[131] Whereas the HTS screen identified 85 compounds with $IC_{50} < 100\ \mu M$, a 0.021% hit rate, the virtual screen identified 365 high-scoring molecules, of which 127 (34.8%) inhibited with $IC_{50} < 100\ \mu M$. The authors acknowledge, however, that the presence of plasma protein in the HTS screen artificially depressed its hit rate, whereas the compounds identified by DOCK were screened in the absence of plasma protein. Even with this bias in favor of the virtual screen, this is still an encouraging result. Ultimately the test for any screening output is the usefulness of the compounds as starting points for a project program, where consideration of ADME properties may well provide part of the selection criteria.

In another example, ligands for factor Xa were selected from a virtual library by using PRO-SELECT. The library of putative ligands had been obtained by enumeration of compounds derived by attachment of a set of substituents around core templates.[132] As a control, a similar sized library was also synthesized, based on reasonable medicinal chemistry principles, but without the application of PRO-SELECT. A tenfold enhancement in activity was claimed for the PRO-SELECT set. Likewise when inhibitors of cathepsin D were derived from a library of compounds, synthesized by parallel methods, and guided by structure-based design, enrichments of two- to sevenfold were found compared to the activities of a similar number of compounds selected from a diverse chemical library.[133]

8. Summary and Outlook

Structure-based drug design has contributed to the discovery of a number of drugs and late-stage clinical candidates. It is now common for a series of ligand–protein structures to be available in discovery projects. Where several ligands have been identified, more information is usually obtained by determining complexes with dissimilar ligands than by determining several in which the ligands are structurally closely related. Perversely, the persuasiveness of structural information allied to seductively high in vitro potency can constitute a barrier in the journey from ligand design to drug discovery. The use of ADME data alongside primary screening is now becoming routine in the pharmaceutical industry. The traditional approach of maintaining or including polar interactions while increasing in vitro potency using hydrophobicity is unacceptable if that is achieved at the expense of other druglike properties.

The availability of X-ray derived structural information on protein–ligand complexes is increasing, and this is a useful tool in lead optimization. However, the ambiguities associated with structural models derived from X-ray data may not be fully appreciated. The process of deriving an atomic model from electron density data disguises uncertainties in the identity and position of ligand, water, and protein atoms. The observed ligand and protein conformation can be affected by crystallization conditions. It can be difficult for even the most conscientious medicinal chemist to avoid drawing misleading conclusions.

These ambiguities have important consequences for the application of structure-based design methodologies. Calculation of binding affinities is currently too imprecise to guide design in the narrow range of affinities observed during the optimization of a lead compound to a drug. The use of docking and scoring tools to design combinatorial chemistry libraries makes some allowance for the inaccuracies of scoring functions, and cases already exist that demonstrate an important complementarity between these technologies. Virtual and property-based screening also has utility for the choice of compound subsets for low-throughput screens, which are not amenable to HTS. The prevalence of induced fit

in ligand–protein interactions also adds complexity to predicting affinities, but at the same time offers new opportunities in ligand design. At present the ability to predict the protein movement and its consequences upon ligand binding is limited. However, it does appear that hydrophobic residues, particularly Phe, Tyr, and Trp and those residues associated with function, are often implicated. In summary, the opportunities for structure-based design have never been greater.

Received: June 5, 2002
Revised: October 2, 2002 [A539]

[1] T. A. Jones, J. Y. Zou, S. W. Cowan, M. Kjeldgaard, *Acta Crystallogr. Sect. A* **1991**, *47*, 110–119.
[2] A. T. Brunger, P. D. Adams, G. M. Clore, W. L. DeLano, P. Gros, R. W. Grosse-Kunstleve, J. S. Jiang, J. Kuszewski, M. Nilges, N. S. Pannu, R. J. Read, L. M. Rice, T. Simonson, G. L. Warren, *Acta. Crystallogr. Sect. D* **1998**, *54*, 905–921.
[3] A. T. Brünger, *" X-PLOR. A System for Crystallography and NMR"*, Yale University, New Haven, CT, USA, **1990**.
[4] Collaborative Computational Project Number 4, *Acta Crystallogr. Sect. D* **1994**, *50*, 760–763.
[5] M. A. Marti-Renom, A. Stuart, A. Fiser, R. Sanchez, F. Melo, A. Sali, *Annu. Rev. Biophys. Biomol. Struct.* **2000**, *29*, 291–325.
[6] C. M. Oshiro, I. D. Kuntz, J. S. Dixon, *J. Comput.-Aided Mol. Des.* **1995**, *9*, 113–130.
[7] M. Rarey, B. Kramer, T. Lengauer, G. Klebe, *J. Mol. Biol.* **1996**, *261*, 470–489.
[8] G. Jones, P. Willett, R. C. Glen, A. R. Leach, R. Taylor, *J. Mol. Biol.* **1997**, *267*, 727–748.
[9] P. J. Goodford, *J. Med. Chem.* **1985**, *28*, 849–857.
[10] A. Miranker, M. Karplus, *Proteins Struct. Funct. Genet.* **1991**, *11*, 29–34.
[11] M. Hendlich, *Acta Crystallogr. Sect. D* **1998**, *54*, 1178–1182.
[12] M. L. Verdonk, J. C. Cole, R. Taylor, *J. Mol. Biol.* **1999**, *289*, 1093–1108.
[13] H. J. Bohm, *J. Comput. -Aided. Mol. Des.* **1994**, *8*, 243–256.
[14] H. Gohlke, M. Hendlich, G. Klebe, *J. Mol. Biol.* **2000**, *295*, 337–356.
[15] A. V. Ishchencko, E. I. Shakhnovich, *J. Med. Chem.* **2002**, *45*, 2770–2780.
[16] P. W. Sprauge, *Perspect. Drug Discovery Des.* **1995**, *3*, 1–20.
[17] R. D. Cramer, D. E. Patterson, J. D. Bunce, *J. Am. Chem. Soc.* **1988**, *110*, 5959–5967.
[18] M. Baroni, G. Constantino, G. Cruciani, D. Riganelli, R. Valigi, S. Clementi, *Quant. Struct.-Act. Relat.* **1993**, *12*, 9–20.
[19] LEAPFROG Tripos Inc., 1699 South Hanley Rd., St Louis, MO, 63144, USA.
[20] B. A. Grzybowski, A. V. Ishenko, J. Shamada, E. I. Shakhnovich, *Acc. Chem. Res.* **2002**, *35*, 261–269.
[21] V. J. Gillet, W. Newell, P. Mata, G. Myatt, S. Sike, Z Zsoldos, A. P. Johnson, *J. Chem. Inf. Comput. Sci.* **1994**, *34*, 207–217.
[22] UNITY 4.2.1 Tripos Inc., 1699 South Hanley Rd., St Louis, MO, 63144, USA.
[23] V. Schnecke, C. A. Swanson, E. D. Getzoff, J. A. Tainer, L. A. Kuhn, *Proteins Struct. Funct. Genet.* **1998**, *33(1)*, 74–87.
[24] S. B. Shuker, P. J. Hajduk, R. P. Meadows, S. W. Fesik, *Science* **1996**, *274*, 1531–1534.
[25] J. Fejzo, C. A. Lepre, J. W. Peng, G. W. Bemis, Ajay, M. A. Murko, J. M. Moore, *Chem. Biol.* **1999**, *6*, 755–769.
[26] V. L. Neinaber, P. L. Richardson, V. Klighofer, J. J. Bouska, V. L. Giranda, J. Greer, *Nat. Biotechnol.* **2000**, *18*, 1105–1108.
[27] T. L. Blundell, H. Joti, C. Abell, *Nat. Rev. Drug Discovery* **2002**, *1*, 145–154.
[28] A. R. Fersht, J. P. Shi, J. Knill-Jones, D. M. Lowe, A. J. Wilkinson, D. M. Blow, P. Brick, Carter, M. M. Y. Waye, G. Winter, *Nature* **1985**, *314*, 235–238.
[29] D. H. Williams, M. S. Searle, J. P. Mackay, U. Gerhard, R. A. Maplestone, *Proc. Natl. Acad. Sci. USA* **1993**, *90*, 1172–1178.
[30] T. G. Davies, J. R. H. Tame, R. E. Hubbard, *Perspect. Drug Discovery Des.* **2000**, *20*, 29–42.
[31] C. A. Lipinski, F. Lombardo, B. W. Dominy, P. J. Feeney, *Adv. Drug Delivery Rev.* **1997**, *23*, 2–25.
[32] Ajay, W. P. Walters, M. A. Murcko, *J. Med. Chem.* **1998**, *41*, 3314–3324.
[33] http://setiathome.ssl.berkeley.edu/.
[34] http://www.chem.ox.ac.uk/curecancer.html.
[35] A. M. Davis, J. Dixon, C. J. Logan, D. W. Payling, in *Pharmacokinetic Challenges in Drug Discovery*, (Eds.: O. Pelkonen, A. Baumann, A. Reichel) Springer, Berlin, **2002**, 1–32.
[36] M. A. Murko, P. R. Caron, P. S. Charifson, *Annu. Rep. Med. Chem.* **1999**, *34*, 297–306.
[37] G. Schneider, H.-J. Bohm, *Drug Discovery Today* **2002**, *7*, 64–70.
[38] R. E. Babine, S. L. Bender, *Chem. Rev.* **1997**, *97*, 1359–1472.
[39] M. Stahl, M. Rarey, G. Klebe, *Methods and Principles in Medicinal Chemistry Volume 14 Bioinformatics—From Genome to Drug*, (Ed.: Thomas Lengauer), Wiley-VCH, **2002**, pp. 137–170.
[40] M. G. Bursavich, D. H. Rich, *J. Med. Chem.* **2002**, *45*, 541–558.
[41] M. T. Huisman, J. W. Smit, H. R. Wiltshire, R. M. W. Hoetelmans, J. H. Beijnen, A. H. Schinkel, *Mol. Pharmacol.* **2001**, *59*, 806–813.
[42] G. C. Williams, P. J. Sinko, *Adv. Drug Delivery Rev.* **1999**, *39*, 211–238.
[43] V. de Lucca, P. Y. S. Lam, *Drugs Future* **1998**, *23*, 987–994.
[44] J. D. Rodgers, P. Y. S. Lam, B. L. Johnson, H. Wang, S. S. Ko, S. P. Seitz, G. L. Trainor, P. S. Anderson, R. M. Klabe, L. T. Bacheler, B. Cordova, S. Garber, C. Reid, M. R. Wright, C.-H. Chang, S. Erickson-Viitanen, *Chem. Biol.* **1998**, *5*, 597–608.
[45] P. A. Aristoff, *Drugs Future* **1998**, *23*, 995–999.
[46] M. von Itzstein, W.-Y. Wu, G. B. Kok, M. S. Pegg, J. C. Dyason, B. Jin, T. V. Phan, M. L. Smythe, H. F. White, S. W. Oliver, P. M. Colman, J. N. Varghese, D. M. Ryan, J. M. Woods, R. C. Bethell, V. J. Hotham, J. M. Cameron, C. R. Penn, *Nature* **1993**, *363*, 418–423.
[47] Physicians' Desk Reference, 55. edition, Thomson Medical Economics, Montvale, **2001**, p. 1454.
[48] C. U. Kim, W. Lew, M. A. Williams, H. Liu, L. Zhang, S. , Swaminathan, N. Bischofberger, M. S. Chen, D. B. Mendel, C. Y. Tai, W. G. Laver, R. C. Stevens, *J. Am. Chem. Soc.* **1997**, *119*, 681–690.
[49] R&D Insight, **2000**, ADIS International Ltd., Chester, United Kingdom.
[50] M. A. Navia, J. P. Springer, M. Poe, J. Boger, K. Hoogsteen, *J. Biol. Chem.* **1984**, *259*, 12714–12717.
[51] A. R. Sielecki, K. Hayakawa, M. Fujinaga, M. E. P. Murphy, M. Frazer, A. K. Muir, C. T. Carilli, J. A. Lewicki, J. D. Baxter, M. N. G. James, *Science* **1989**, *243*, 1341–1351.
[52] M. A. Navia, P. R. Chaturvedi, *Drug Discovery Today* **1996**, *1*, 179–189.
[53] C. Oefner, A. Binggeli, V. Breu, D. Bur, J.-P. Clozel, A. D′Arcy, A. Dorn, W. Fischli, F. Gruninger, R. Guller, G. Hirth, H. P. Marki, S. Mathews, M. Miuller, R. G. Ridley, H. Stadler, E. Viera, M. Wilhelm, F. K. Winkler, W. Wostl, *Chem. Biol.* **1999**, *6*, 127–131.
[54] H. Kubinyi, *J. Recept. Signal Transduction Res.* **1999**, *19*, 15–39.
[55] J. Greer, J. W. Erickson, J. J. Baldwin, M. D. Varney, *J. Med. Chem.* **1994**, *37*, 1035–1054.
[56] G. S. Ponticello, M. F. Sugre, B. Plazonnet, G. Durand-Cavagna, *Pharm. Biotechnol.* **1998**, *11*, 555–574.

[57] R. W. Schevitz, N. J. Bach, D. G. Carlson, N. Y. Chirgadze, D. K. Clawson, R. D. Dillard, S. E. Draheim, L. W. Hartley, N. D. Jones, E. D. Mihelich, J. L. Olkowski, D. W. Snyder, C. Sommers, J.-P. Wery, *Nat. Struct. Biol.* **1995**, *2*, 458 – 465.
[58] E. D. Mihelich, R. W. Schevitz, *Biochim. Biophys. Acta* **1999**, *1441*, 223 – 228.
[59] J. Drenth, *Principles of Protein X-ray Crystallography*, Springer-Verlag, New York, **1994**.
[60] T. A. Jones, M. Kjeldgaard, *Methods Enzymol.* **1997**, *277*, 173 – 208.
[61] G. J. Kleywegt, T. A. Jones, *Methods Enzymol.* **1997**, *277*, 208 – 230.
[62] a) F. C. Bernstein, T. F. Koetzle, G. J. B. Williams, E. F. Meyer, Jr., M. D. Brice, J. R. Rodgers, O. Kennard, T. Shimanouchi, M. Tasumi, *J. Mol. Biol.* **1977**, *112*, 535 – 542; b) http://www.rcsb.org/pdb.
[63] G. J. Kleywegt, *Acta Crystallogr. Sect. D* **2000**, *56*, 249 – 265.
[64] G. J. Kleywegt, T. A. Jones in *Making the Most of Your Model* (Eds.: W. N. Hunter, J. M. Thornton, S. Bailey), SERC Daresbury Laboratory, Warrington, **1995**, pp. 11 – 24.
[65] C. I. Brändén, T. A. Jones, *Nature* **1990**, *343*, 687 – 689.
[66] M. A. Hanson, T. K. Oost, C. Sukonpan, D. H. Rich, R. C. Stevens, *J. Am. Chem. Soc.* **2000**, *122*, 11268 – 11269.
[67] M. A. Hanson, T. K. Oost, C. Sukonpan, D. H. Rich, R. C. Stevens, *J. Am. Chem. Soc.* **2002**, *124*, 10248.
[68] A. T. Brünger, *Nature* **1992**, *355*, 472 – 475.
[69] G. J. Kleywegt, T. A. Jones, *Structure* **1995**, *3*, 535 – 540.
[70] A. T. Brünger, *Methods Enzymol.* **1997**, *277*, 366 – 396.
[71] G. J. Kleywegt, A. T. Brünger, *Structure* **1996**, *4*, 897 – 904.
[72] R. W. W. Hooft, G. Vriend, C. Sander, E. E. Abola, *Nature* **1996**, *381*, 272.
[73] http://www.cmbi.kun.nl/gv/pdbreport.
[74] J. Y. Zou, M. R. Harris, T. Taylor, A. Wählby, G. J. Kleywegt, T. A. Jones, unpublished results.
[75] J. F. Leszczynski, G. D. Rose, S. Milton, *Science* **1986**, *234*, 849 – 855.
[76] B. Hao, W. Gong, T. K. Ferguson, M. Carey, J. A. Krzycki, M. K. Chan, *Science* **2002**, *296*, 1462 – 1466.
[77] G. J. Kleywegt, T. Bergfors, H. Senn, P. Le Motte, B. Gsell, K. Shudo, T. A. Jones, *Structure* **1994**, *2*, 1241 – 1258.
[78] A. Fersht, *Enzyme Structure and Mechanism*, Freeman, New York, **1985**, pp. 155 – 175.
[79] G. Klebe, M. Bohm, F. Dullweber, U. Gradler, H. Gohlke, M. Hendlich, in *Molecular Modelling and Prediction of Bioactivity* (Eds.: K. Gundertofte, F. S. Jorgensen), Kluwer/Plenum, New York, **2000**, pp. 103 – 110.
[80] M. T. Stubbs, S. Reyda, F. Dullweber, M. Moller, G. Klebe, D. Dorsch, W. W. K. R. Mederski, H. Wurziger, *Chembiochem* **2002**, *3*, 246 – 249.
[81] S. M. Cutfield, E. J. Dodson, B. F. Anderson, P. C. E. Moody, C. J. Marshall, P. A. Sullivan, J. F. Cutfield, *Structure* **1995**, *3*, 1261 – 1271.
[82] C. Abad-Zapatero, R. Goldman, S. W. Muchmore, C. Hutchins, K. Stewart, J. Navaza, C. D. Payne, T. L. Ray, *Protein Sci.* **1996**, *5*, 640 – 652.
[83] V. Nahoum, G. Roux, V. Anton, P. Rouge, A. Puigserver, H. Bischoff, B. Henrissat, F. Payan, *Biochem. J.* **2000**, *346*, 201 – 208.
[84] Y. So, M. M. Yamashita, S. E. Greasley, C. A. Mullen, J. H. Shim, P. A. Jennings, S. J. Benkovic, L. A. Wilson, *J. Mol. Biol.* **1998**, *281*, 485 – 499.
[85] O. Mayans, M. Scott, I. Connerton, T. Gravesen, J. Benen, J. Visser, R. Rickersgill, J. Jenkins, *Structure* **1997**, *5*, 677 – 689.
[86] K. Matsuda, K. Mizuguchi, T. Nishioka, H. Kato, N. Go, J. Oda, *Protein Eng.* **1996**, *9*, 1083 – 1092.
[87] "Options for the Control of Influenza IV": A. Harris, F. Forouhar, S. Qiu, S. Shihong, L. M. Bingdong, Int. Congress Series, **2001**, *1219*, 405 – 410.
[88] R. Berisio, F. Sica, V. S. Lamzin, K. S. Wilson, A. Zagari, L Mazzarella, *Acta Crystallogr. Sect. D* **2002**, *58*, 441 – 450.
[89] S. Daopin, D. R. Davies, *Acta Crystallogr. Sect. D* **1994**, *50*, 85 – 92.
[90] D. H. Ohlendorf, *Acta Crystallogr. Sect. D* **1994**, *50*, 808 – 812.
[91] B. A. Fields, H. H. Bartsch, H. D. Bartunik, F. Cordes, J. M. Guss, H. C. Freeman, *Acta Crystallogr. Sect. D* **1994**, *50*, 709 – 730.
[92] J. E. Ladbury, *Chem. Biol.* **1996**, *3*, 973 – 980.
[93] J. Boström, *J. Comp-Aided Mol. Des.* **2001**, *15*, 1137 – 1152.
[94] G. J. Kleywegt, T. A. Jones, *Acta Crystallogr. D* **1998**, *54*, 1119 – 1131.
[95] http://xray.bmc.uu.se/hicup.
[96] D. M. F. van Aalten, R. Bywater, J. B. C. Findlay, M. Hendlich, R. W. W. Hooft, G. Vriend, *J. Comput. Aided Mol. Des.* **1996**, *10*, 255 – 262.
[97] J. Eads, J. C. Sacchettini, A. Kromminga, J. I. Gordon, *J. Biol. Chem.* **1993**, *268*, 26375 – 26385.
[98] J. Thompson, N. Winter, D. Terwey, J. Bratt, L. Banaszak, *J. Biol. Chem.* **1997**, *272*, 7140 – 7150.
[99] M. G. Jakoby, K. R. Miller, J. J. Toner, A. Bauman, L. Cheng, E. Li, D. P. Cistola, *Biochemistry* **1993**, *32*, 872 – 878.
[100] J. W. M. Nissink, C. Murray, M. Hartshorn, M. L Verdonk, J. C. Cole, R. Taylor, *Proteins Struct. Funct. Genet.* **2002**, *49*, 457 – 471.
[101] E. E. Abola, A. Bairoch, W. C. Barker, S. Beck, D. A. Benson, H. Berman, G. Cameron, C. Cantor, S. Doubet, T. J. P. Hubbard, T. A. Jones, G. J. Kleywegt, A. S. Kolastar, A. Van Kuik, A. M. Lest, H.-W. Mewes, D. Neuhaus, F. Pfeiffer, L. F. TenEyck, R. J. Simpson, G. Stoesser, J. L. Sussman, Y. Tateno, A. Tsugita, E. L. Ulrick, J. F. G. Vliegenthart, *Bio-Essays* **2000**, *22*, 1024 – 1034.
[102] http://www.expasy.ch/spdbv.
[103] G. J. Kleywegt, T. A. Jones, *Structure*, **2002**, *10*, 465 – 472.
[104] http://fsrv1.bmc.uu.se/eds.
[105] http://xray.bmc.uu.se/embo2001/modval.
[106] E. M. S. Harris, A. E. Aleshin, L. M. Firsov, R. B. Honzatko, *Biochemistry* **1993**, *32*, 1618 – 1626.
[107] M. J. Boulanger, M. E. P. Murphy, *Biochemistry* **2001**, *40*, 9132 – 9141.
[108] P. C. Sanschagrin, L. A. Kuhn, *Protein Sci.* **1998**, *7*, 2054 – 2064.
[109] http://www.ccdc.cam.ac.uk/prods/gold/value.html.
[110] C. W. Murray, C. A. Baxter, A. D. Frenkel, *J. Comput.-Aided Mol. Des.* **1999**, *13*, 547 – 562.
[111] C. Hansch, *Acc. Chem. Res.* **1993**, *26*,147 – 153.
[112] C. Hansch, D. Hoekman, H. Gao, *Chem. Rev.* **1996**, *96*, 1045 – 1075.
[113] D. H. Williams, M. S. Westwell, *Chem. Soc. Rev.* **1998**, *27*, 57 – 64.
[114] I. P. Street, C. R. Armstrong, S. G. Withers, *Biochemistry* **1986**, *25*, 6021 – 6027.
[115] I. Muegge, Y. C. Martin, *J. Med. Chem.* **1999**, *42*, 791 – 804.
[116] H.-J. Bohm, M. Stahl, *Med. Chem. Res.* **1999**, *9*, 445 – 462.
[117] R. D. Head, M. L. Smythe, T. I. Oprea, C. L. Waller, S. M. Green, G. R. Marshall, *J. Am. Chem. Soc.* **1996**, *118*, 3959 – 3969.
[118] T. I. Oprea, G. R. Marshall, *Perspect. Drug Discovery Des.* **1998**, *9–11*, 35 – 61.
[119] M. K. Holloway, J. M. Wai, T. A. Halgren, P. M. D. Fitzgerald, J. P. Vacca, B. D. Dorsey, R. B. Levin, W. J. Thompson, L. J. Chen, S. J. deSolms, N. Gaffin, A. K. Ghosh, E. A. Giuliani, S. L. Graham, J. P. Guare, R. W. Hungate, T. A. Lyle, W. M. Sanders, T. J. Tucker, M. Wiggins, C. M. Wiscount, O. W.

Woltersdorf, S. D. Young, P. L. Darke, J. A. Zugay, *J. Med. Chem.* **1995**, *38*, 305 – 317.
[120] A. M. Davis, S. J. Teague, *Angew. Chem.* **1999**, *111*, 778 – 792; *Angew. Chem. Int. Ed.* **1999**, *38*, 736 – 749.
[121] R. Najmanovich, J. Kuttner, V. Sobolev, M. Edelman, *Proteins Struct. Funct. Genet.* **2000**, *39*, 261 – 268.
[122] P. Goodford, *Alfred Benzon Symp.* **1998**, *42*, 215 – 230.
[123] V. Schnecke, L. Kuhn, *Perspect. Drug Discovery Des.* **2000**, *20*, 171 – 190.
[124] A. C. Anderson, R. H. O'Neil, T. S. Surti, R. M. Stroud, *Chem. Biol.* **2001**, *8*, 445 – 457.
[125] D. Joseph-McCarthy, S. K. Tsang, D. J. Filman, J. M. Hogle, M. Karplus, *J. Am. Chem. Soc.* **2001**, *123*, 12758 – 12769.
[126] A. Rockwell, M. Melden, R. A. Copeland, K. Hardman, C. P. Decicco, W. F. DeGrado, *J. Am. Chem. Soc.* **1996**, *118*, 10337 – 10338.
[127] A. M. Davis, T. I. Oprea, S. J. Teague, P. D. Leeson, *Angew. Chem.* **1999**, *111*, 3962 – 3967; *Angew. Chem. Int. Ed.* **1999**, *38*, 3743 – 3748.
[128] T. I. Oprea, A. M. Davis, S. J. Teague, P. D. Leeson, *J. Chem. Inf. Comput. Sci.* **2001**, *41*, 1308 – 1315.
[129] M. Hann, A. R. Leach, . G. Harper, *J. Chem. Inf. Comput. Sci.* **2001**, *41*, 856 – 864.
[130] T. J. Stout, C. R. Sage, R. M. Stroud, *Structure* **1998**, *6*, 839 – 848.
[131] T. N. Doman, S. L. McGovern, B. J. Witherbee, T. P. Kasten, R. Kurumbail, W. C. Stallings, D. T. Connolly, B. K. Shoichet, *J. Med. Chem.* **2002**, *45*, 2213 – 2221.
[132] J. W. Leibeshuetz, S. D. Jones, P. J. Morgan, C. W. Murray, A. D. Rimmer, J. M. E. Roscoe, B. Waszkowycz, P. M. Welsh, W. A. Wylie, S. C. Young, H. Martin, J. Mahler, L. Brady, K. Wilkinson, *J. Med. Chem.* **2002**, *45*, 1221 – 1232.
[133] E. K. Kick, D. C. Roe, A. G. Skillman, G. Lui, T. J. A. Ewing, Y. Sun, I. D. Kuntz, J. A. Ellman, *Chem. Biol.* **1997**, *4*, 297 – 307.